

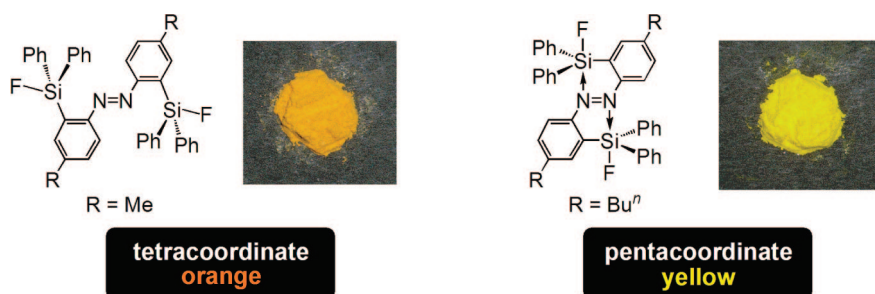
## Crucial Role of N $\cdots$ Si Interactions in the Solid-State Coloration of Disilylazobenzenes

Masaki Yamamura,<sup>†</sup> Naokazu Kano,<sup>†</sup> Takayuki Kawashima,<sup>\*,†</sup> Tomonari Matsumoto,<sup>‡</sup>  
Jun Harada,<sup>‡</sup> and Keiichiro Ogawa<sup>\*,‡</sup>

Department of Chemistry, Graduate School of Science, The University of Tokyo, 7-3-1 Hongo, Bunkyo-ku, Tokyo 113-0033, Japan, and Department of Basic Science, Graduate School of Arts and Sciences, The University of Tokyo, 3-8-1 Komaba, Meguro-ku, Tokyo 153-8902, Japan

takayuki@chem.s.u-tokyo.ac.jp; ogawa@ramie.c.u-tokyo.ac.jp

Received June 24, 2008



2,2'-Bis(fluorodiphenylsilyl)azobenzenes bearing two methyl and butyl groups at the 4- and 4'-positions were synthesized, and their X-ray crystallographic analyses revealed that they have tetracoordinated and pentacoordinated silicon atoms, respectively. Although the two compounds showed almost the same spectra in solution, the reflectance spectra of the solid revealed that the pentacoordinated state had a weaker absorbance in the long-wavelength region compared with that of the tetracoordinated state, which is ascribed to the shift of the n- $\pi^*$  transition. This difference in the absorptions due to the n- $\pi^*$  transition drastically affects the color of the azobenzenes: the color of the pentacoordinated state becomes apparently paler than that of the tetracoordinated state.

### Introduction

One of the main topics in silicon chemistry is the highly coordinated organosilicon compounds,<sup>1</sup> whose specific dative bonding and high reactivity have attracted many researchers.<sup>2</sup> Many pentacoordinated organosilicon compounds with an intramolecular dative N $\cdots$ Si bond<sup>3</sup> equilibrate with the tetra-coordinated species in solution because the dative bond is weak and easily dissociated. Since the dative bond also changes the structure around the silicon atom, formation of the pentacoor-

ordinated states will be useful for change of several properties. However, there is almost no report of change in the optical, electronic, and magnetic properties of the organosilicon compounds caused by the N $\cdots$ Si dative bond.<sup>4</sup> We previously

<sup>†</sup> Department of Chemistry, The University of Tokyo.

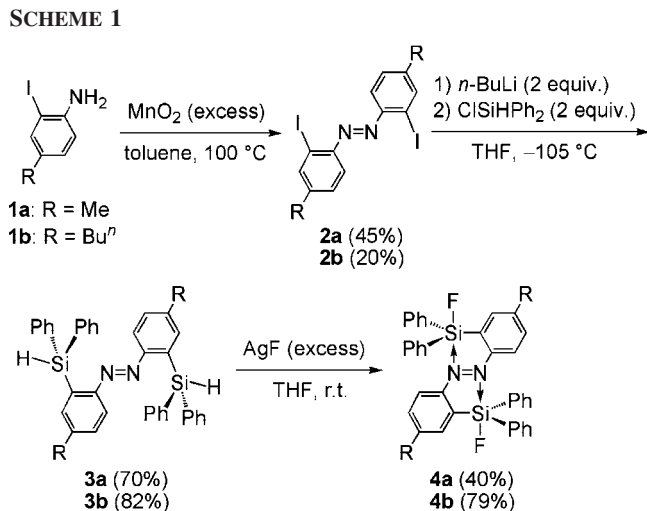
<sup>‡</sup> Department of Basic Science, The University of Tokyo.

(1) (a) Corriu, R. J. P.; Young, J. C. In *The Chemistry of Organic Silicon Compounds*; Patai, S., Rappoport, Z., Eds.; Wiley: New York, 1989; Chapter 20, p 1241. (b) Holmes, R. R. *Chem. Rev.* **1990**, *90*, 17–31. (c) Chuit, C.; Corriu, R. J. P.; Reye, C.; Young, J. C. *Chem. Rev.* **1993**, *93*, 1371–1448. (d) Holmes, R. R. *Chem. Rev.* **1996**, *96*, 927–950. (e) Kost, D.; Kalikhman, I. In *The Chemistry of Organic Silicon Compounds*; Patai, S., Rappoport, Z., Eds.; Wiley: New York, 1998; Vol. 2, p 1339. (f) Chuit, C.; Corriu, R. J. P.; Reye, C.; Young, J. C. In *Chemistry of Hypervalent Compounds*; Akiba, K.-y., Ed.; Wiley-VCH: New York, 1999; p 81. (g) Kira, M.; Zhang, L.-C. In *Chemistry of Hypervalent Compounds*; Akiba, K.-y., Ed.; Wiley-VCH: New York, 1999; p 147. (h) Abele, E. *Main Group Met. Chem.* **2005**, *28*, 45.

(2) Recent reports: (a) Wagler, J.; Doert, T.; Roewer, G. *Angew. Chem., Int. Ed.* **2004**, *43*, 2441–2444. (b) Wagler, J.; Böhme, U.; Brendler, E.; Roewer, G. *Organometallics* **2004**, *23*, 6066–6069. (c) Gostevskii, B.; Kalikhman, I.; Tessier, C. A.; Panzner, M. J.; Youngs, W. J.; Kost, D. *Organometallics* **2005**, *24*, 2913–2920. (d) Gostevskii, B.; Kalikhman, I.; Tessier, C. A.; Panzner, M. J.; Youngs, W. J.; Kost, D. *Organometallics* **2005**, *24*, 5786–5788. (e) Gerlach, D.; Brendler, E.; Heine, T.; Wagler, J. *Organometallics* **2007**, *26*, 234–240. (f) Kalikhman, I.; Gostevskii, B.; Kertsus, E.; Botoshansky, M.; Tessier, C. A.; Youngs, W. J.; Deuerlein, S.; Stalke, D.; Kost, D. *Organometallics* **2007**, *26*, 2652–2658. (g) Wagler, J.; Hill, A. F. *Organometallics* **2007**, *26*, 3630–3632.

(3) (a) Helmer, B. J.; West, R.; Corriu, R. J. P.; Poirier, M.; Royo, G.; de Saxcé, A. *J. Organomet. Chem.* **1983**, *251*, 295–298. (b) Wagler, J.; Böhme, U.; Brendler, E.; Roewer, G. *Organometallics* **2005**, *24*, 1348–1350. (c) Gostevskii, B.; Silbert, G.; Ahear, K.; Sivaramakrishna, A.; Stalke, D.; Deuerlein, S.; Kocher, N.; Voronkov, M. G.; Kalikhman, I.; Kost, D. *Organometallics* **2005**, *24*, 2913–2920. (d) Kalikhman, I.; Gostevskii, B.; Botoshansky, M.; Kaftory, M.; Tessier, C. A.; Panzner, M. J.; Youngs, W. J.; Kost, D. *Organometallics* **2006**, *25*, 1252–1258. (e) Gostevskii, B.; Zamstein, N.; Korlyukov, A. A.; Baukov, Y. I.; Botoshansky, M.; Kaftory, M.; Kocher, N.; Stalke, D.; Kalikhman, I.; Kost, D. *Organometallics* **2006**, *25*, 5416–5423.

## SCHEME 1



reported the syntheses and properties of azobenzenes bearing a silicon atom at the 2-position and switched their coordination states by using their *E*-*Z* photoisomerization.<sup>5</sup> Some of the organosilicon compounds bearing an azobenzene moiety could form a pentacoordinated state with a dative bond from a nitrogen atom of the azo group to the silicon atom, which showed yellow color in solution in contrast to reddish orange in usual azobenzene.<sup>5d</sup> Azobenzene analogues strongly absorb visible light, and their colored character has been used as dyes, i.e., azo dye.<sup>6</sup> Their color originates with their  $n-\pi^*$  and/or  $\pi-\pi^*$  absorption bands. One of the most useful methods to change the color of azobenzene derivatives is to perturb the frontier orbitals such as  $n$ ,  $\pi$ , and  $\pi^*$  orbitals by substitution on the two benzene rings with electron-donating or electron-withdrawing groups. Another conceivable method is utilization of some interactions between a nitrogen atom and another atom nearby. The difference in the color between azobenzene and the 2-silylazobenzenes was apparently ascribed to the perturbation by the  $N\cdots Si$  coordination and/or the substituent effect by the silyl group through  $\pi$ -bonds. However, it is not clear how they affect the color of azobenzenes because both the tetra- and pentacoordinated states that may have different  $\pi$ -electron systems exist in solution. Therefore, the effect of the  $N\cdots Si$  coordination is not distinguishable from the substituent effect in solution. If the two isomers of an azobenzene bearing the same silyl group with and without the interaction are separated, the difference in their color will be elucidated. In this paper, we report the isolation of 2,2'-bis(fluorodiphenylsilyl)azobenzenes bearing two methyl or butyl groups at the 4- and 4'-positions as the tetracoordinated form or the pentacoordinated form, respectively. We show how the colors of the disilylazobenzenes are perturbed by the  $N\cdots Si$  interactions on the basis of the study of their structures and the colors in the solid state, where there is no interconversion between the pentacoordinated and the tetracoordinated states.

(4) (a) Wagler, J.; Roewer, G. *Z. Naturforsch. B* **2005**, *60*, 709–714. (b) Wagler, J.; Gerlach, D.; Böhme, U.; Roewer, G. *Organometallics* **2006**, *25*, 2929–2933. (c) Wagler, J.; Roewer, G. *Inorg. Chim. Acta* **2007**, *360*, 1717–1724. (5) (a) Kano, N.; Komatsu, F.; Kawashima, T. *Chem. Lett.* **2001**, 338–339. (b) Kano, N.; Komatsu, F.; Kawashima, T. *J. Am. Chem. Soc.* **2001**, *123*, 10778–10779. (c) Kano, N.; Yamamura, M.; Komatsu, F.; Kawashima, T. *J. Organomet. Chem.* **2003**, *686*, 192–197. (d) Kano, N.; Komatsu, F.; Yamamura, M.; Kawashima, T. *J. Am. Chem. Soc.* **2006**, *128*, 7097–7109. (e) Yamamura, M.; Kano, N.; Kawashima, T. *J. Organomet. Chem.* **2007**, *692*, 313–325. (f) Yamamura, M.; Kano, N.; Kawashima, T. *Tetrahedron Lett.* **2007**, *48*, 4033–4036. (6) Zollinger, H. *Color Chemistry*, 3rd ed.; Wiley-VCH: Switzerland, 2003.

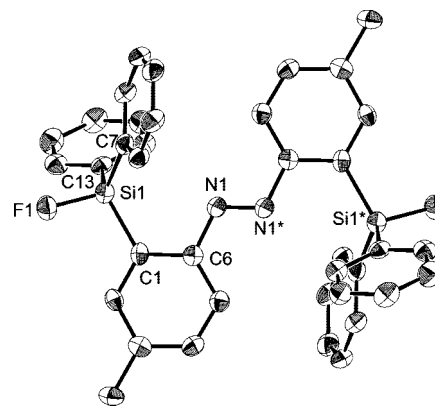


**FIGURE 1.** ORTEP drawing of **4a** (50% probability). Hydrogen atoms were omitted for clarity. Selected bond lengths [Å] and angles [deg] and a torsion angle [deg]: Si1–F1, 1.609(1); Si1–C1, 1.877(2); Si1–C7, 1.863(2); Si1–C13, 1.862(2); N1–N1\*, 1.257(3); F1–Si1–C1, 103.73(7); F1–Si1–C7, 107.57(8); F1–Si1–C13, 104.56(8); C1–Si1–C7, 114.74(8); C1–Si1–C13, 114.23(8); C7–Si1–C13, 110.98(8); N1\*–N1–C6–C1, 167.0(2).

## Results and Discussion

Similarly to the synthetic method for 2-silylazobenzenes,<sup>5d</sup> 2,2'-bis(fluorodiphenylsilyl)azobenzenes **4a** and **4b** were synthesized from the corresponding 2,2'-diiodoazobenzenes (Scheme 1). The crystal structures of **4a** and **4b** were determined by X-ray crystallographic analyses (Figures 1 and 2, respectively).<sup>7</sup>

In single crystals, the N1\* atom is directed to the Si1 atom in **4b** within a short interatomic N1 $\cdots$ Si1 distance (2.467(2) Å)<sup>8</sup> like 2-(fluorodiphenylsilyl)azobenzene (**5**),<sup>5d</sup> but that is not the case in **4a**. The crystal structures clearly indicate the absence and presence of the  $N\cdots Si$  coordination in **4a** and **4b**, respectively. The bond angles (F1–Si1–C, 98.47(6)–100.19(6)°; C–Si1–C, 111.41(7)–120.32(7)°) suggest a distorted trigonal bipyramidal structure around the silicon atom of (*E*)-**4b**, whereas those around the silicon atom (103.73(7)–114.74(8)°) in (*E*)-**4a** suggest that (*E*)-**4a** should be regarded as tetrahedral structure around their silicon atom. The slightly longer Si1–F1 bond length of (*E*)-**4b** (1.637(1) Å) than that of (*E*)-**4a** (1.609(1) Å) is consistent with common tendency of apical bonds composed by 3-center-4-electron bond in trigonal bipyramidal structure.

The single crystals of each **4a** and **4b** were ground to powder, and subsequently, the MAS solid-state <sup>29</sup>Si NMR spectra of the powder of **4a** and **4b** were measured to reveal the coordination states of the silicon atoms. The chemical shift ( $\delta_{Si}$  –4.9) of **4a** in the solid state was almost the same as that ( $\delta_{Si}$  –4.7) of fluorotriphenylsilane in solution,<sup>9</sup> but that ( $\delta_{Si}$  –29.0) of **4b** showed an upfield shift by over 20 ppm, which is generally shown in pentacoordinated silicon compounds.<sup>10</sup> These results and the X-ray crystal structure lead to the conclusion that **4a**

(7) Crystal data for **4a**. C<sub>38</sub>H<sub>32</sub>N<sub>2</sub>F<sub>2</sub>Si<sub>2</sub>, *M* = 610.84, triclinic, space group *P*-1, *Z* = 1,  $\mu$  = 0.159 cm<sup>-1</sup>, *a* = 7.916(4) Å, *b* = 8.961(4) Å, *c* = 11.390(5) Å,  $\alpha$  = 92.725(6)°,  $\beta$  = 105.385(6)°,  $\gamma$  = 97.941(6)°, *V* = 768.5(6) Å<sup>3</sup>, *R*<sub>1</sub> = 0.0369 for 4942 (*I* > 2 $\sigma$ (*I*)) reflections, *wR*<sub>2</sub> = 0.1092 (all data). Crystal data for **4b**. C<sub>44</sub>H<sub>44</sub>N<sub>2</sub>F<sub>2</sub>Si<sub>2</sub>, *M* = 694.99, triclinic, space group *P*-1, *Z* = 2,  $\mu$  = 0.139 cm<sup>-1</sup>, *a* = 10.851(4) Å, *b* = 11.525(4) Å, *c* = 15.430(5) Å,  $\alpha$  = 95.857(4)°,  $\beta$  = 100.122(4)°,  $\gamma$  = 99.054(4)°, *V* = 1859.1(10) Å<sup>3</sup>, *R*<sub>1</sub> = 0.0319 for 1999 (*I* > 2 $\sigma$ (*I*)) reflections, *wR*<sub>2</sub> = 0.0858 (all data). CCDC-648142 (**4a**) and CCDC-648143 (**4b**)

(8) In single crystals of **4b**, there are two independent molecules in the unit cell, and they are almost the same structure except for the conformation of their butyl groups.

(9) (a) Harris, R. K.; Jones, J.; Ng, S. *J. Magn. Reson.* **1978**, *30*, 521. (b) Cella, J. A.; Cargioli, J. D.; Williams, E. A. *J. Organomet. Chem.* **1980**, *186*, 13.

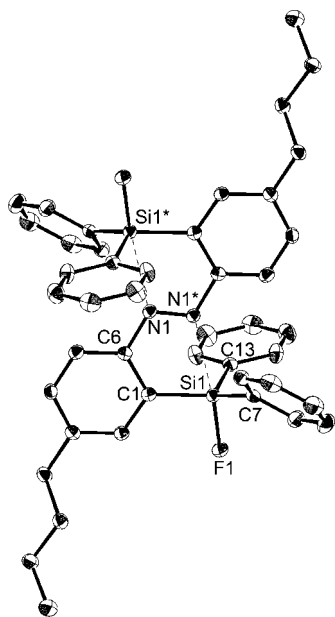


**FIGURE 2.** ORTEP drawing of one of the two independent molecules of **4b** (50% probability). Hydrogen atoms were omitted for clarity. Selected bond lengths [Å] and angles [deg] and a torsion angle [deg]: N1 $\cdots$ Si1\*, 2.467(2); Si1–F1, 1.637(1); Si1–C1, 1.867(2); Si1–C7, 1.866(2); Si1–C13, 1.865(2); N1–N1\*, 1.264(2); F1–Si1–C1, 100.19(6); F1–Si1–C7, 98.47(6); F1–Si1–C13, 99.95(6); C1–Si1–C7, 120.22(6); C1–Si1–C13, 111.41(7); C7–Si1–C13, 120.32(7); N1\*–N1–C6–C1, 0.3(2).

and **4b** have the tetracoordinated and pentacoordinated silicon states in the solid, respectively.

In CDCl<sub>3</sub> solution, the <sup>1</sup>H, <sup>13</sup>C, <sup>19</sup>F, and <sup>29</sup>Si NMR spectra of **4a** and **4b** were almost the same except for the signals due to the methyl and butyl moieties. In the <sup>29</sup>Si NMR spectra at 20 °C, **4a** and **4b** showed at  $\delta_{\text{Si}}$  –21.0 and –20.3, respectively, both of which are apparently different from their chemical shifts in the solid state, indicating the presence of the equilibrium in solution. The equilibrium is confirmed by the significant temperature dependence of the  $\delta_{\text{Si}}$  of **4b** in CD<sub>2</sub>Cl<sub>2</sub> ( $\delta_{\text{Si}}$  (–100 °C) –28.8;  $\delta_{\text{Si}}$  (–40 °C) –26.7;  $\delta_{\text{Si}}$  (20 °C) –21.4).<sup>11</sup> Assuming that the equilibrium is composed of the only two isomers, the equilibrium constants were calculated from the observed chemical shifts as the weighted average of the penta- and tetracoordinated state (see Supporting Information).<sup>3a</sup> The equilibrium constant of **4b** in CD<sub>2</sub>Cl<sub>2</sub> is estimated to be 2.2 at 20 °C, and therefore the pentacoordinated state exists twice as much as the tetracoordinated state.

The UV–vis absorption spectra of **4a** and **4b** in dichloromethane are almost the same (Figure 3). Each of these spectra is of the equilibrium mixture of the tetracoordinated and the pentacoordinated forms with an approximate molar ratio of 2:1, as shown by the <sup>29</sup>Si NMR spectra. There is a strong absorption band with  $\lambda_{\text{max}}$  = 380 nm, which is assigned to  $\pi$ – $\pi^*$  transition. This band is appreciably red-shifted compared to the corresponding band of azobenzene ( $\lambda_{\text{max}}$  = 318 nm). The red shift as large as 60 nm is ascribed to the fluorodiphenylsilyl groups at 2- and 2'-positions of the benzene rings, because the bathochromic effect of alkyl groups on azobenzenes is only as

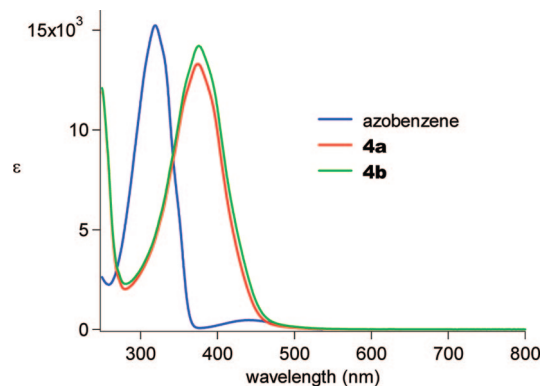


**FIGURE 3.** UV–vis absorption spectra of azobenzene (blue line), **4a** (red line), and **4b** (green line) in dichloromethane at room temperature.

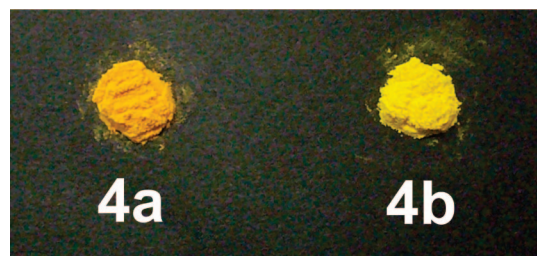


**FIGURE 4.** Colors of **4a** and **4b**.

large as 20 nm in magnitude.<sup>12</sup> The  $n$ – $\pi^*$  band is not observed in the visible region. This is probably because the  $n$ – $\pi^*$  band overlaps with the strong  $\pi$ – $\pi^*$  band, the tail of which extends to 500 nm.

The colors of **4a** and **4b** in dichloromethane are both yellow, which is markedly different from reddish orange of azobenzene. This difference in color is explained by these absorption spectra. In the absorption spectrum of azobenzene, the  $\pi$ – $\pi^*$  band is in the UV region and the  $n$ – $\pi^*$  band in the visible region. The  $n$ – $\pi^*$  band extends to 535 nm and is responsible for the reddish orange.<sup>6</sup> For **4a** and **4b**, the strong  $\pi$ – $\pi^*$  band, which extends to 500 nm, is responsible for their yellow color. This means that the colors of **4a** and **4b** are dominated by the  $\pi$ – $\pi^*$  absorption, whereas the color of azobenzene is dominated by the  $n$ – $\pi^*$  absorption. Although the  $\pi$ – $\pi^*$  bands of **4a** and **4b** are substantially red-shifted compared with that of azobenzene, they lie in the considerably shorter wavelength region than the  $n$ – $\pi^*$  band of azobenzene. As a result, **4a** and **4b** are paler than azobenzene, despite a substantial bathochromic effect of their strongest absorption band, i.e., the  $\pi$ – $\pi^*$  band.

In contrast to the solutions, the colors of **4a** and **4b** in the solid state are noticeably different from each other; **4a** is orange, but **4b** is yellow (Figure 4). They are also different from the reddish orange of azobenzene. This difference in color can be understood in terms of the diffuse reflectance spectra of the powdered samples (Figure 5). A rapid decrease of the reflectance of **4a** and **4b** begins in the wavelength region shorter than 560 and 530 nm, respectively, whereas that of azobenzene begins at further longer wavelength of 590 nm. Thus, the wavelength of the absorption edge increases in the order of **4b**, **4a**, and azobenzene. Their color becomes deeper in this order.

(10) Williams, E. A.; Cargioli, J. D. In *Annual Report on NMR Spectroscopy*; Academic Press: New York, 1979; Vol. 9.

(11) In the <sup>29</sup>Si NMR spectral measurement of **4a**, the S/N ratio was not good owing to its low solubility. The measurement of **4b** alone was sufficient for the further discussion.

(12) (a) Suzuki, H. In *Electronic Absorption Spectra and Geometry of Organic Molecules*; Academic Press: New York, 1967; p 514. (b) Grammaticakis, P. *Bull. Soc. Chim. Fr.* **1951**, 18, 951.



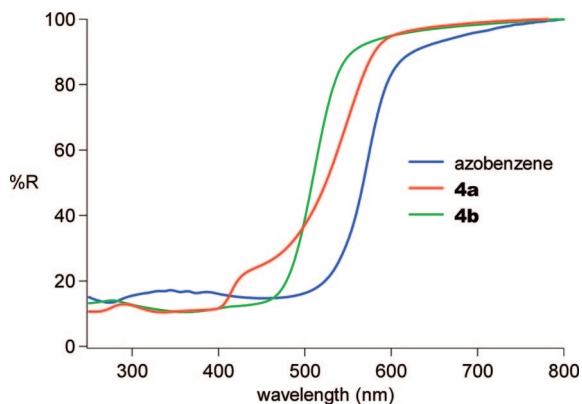


**FIGURE 5.** Diffuse reflectance spectra of azobenzene (blue line), **4a** (red line), and **4b** (green line) at room temperature.

**TABLE 1.** Calculated Chromaticity Coordinates and Corresponding Colors of the Powder of Disilylazobenzenes **4a** and **4b** and Azobenzene

compound	chromaticity coordinate (x, y)	corresponding color	perceived color
azobenzene	0.478, 0.384	orange/pink <sup>a</sup>	reddish orange
<b>4a</b>	0.422, 0.411	yellowish orange	yellowish orange
<b>4b</b>	0.429, 0.464	yellow	yellow

<sup>a</sup> The coordinates lie on the boundary between the two colors.

That the diffuse reflectance spectra correctly reflect the actual color was quantitatively confirmed by the use of the chromaticity coordinate of the powders of the compounds, which is a numerical representation of the color.<sup>13</sup> Their coordinates and corresponding color<sup>14</sup> are listed in Table 1. The coordinates of **4a**, **4b**, and azobenzene lie in the region of yellowish orange, yellow, and the boundary between orange and pink, respectively. Each of these colors agrees well with the perceived color of the corresponding compounds.

The above results show that difference in the diffuse reflectance spectra of **4a** and **4b** can explain the difference in their perceived colors. The deeper color of **4a** is therefore due to the fact that the reflectance of **4a** is smaller than that of **4b** in the wavelength region of 500–600 nm.

To relate the difference in diffuse reflectance spectra to that in absorption bands corresponding to electronic transitions between molecular orbitals, the Kubelka–Munk spectra were obtained for the samples in which the powder is diluted with barium sulfate (Figure 6).<sup>15</sup> The Kubelka–Munk spectra are significantly different between **4a** and **4b**. Their spectra are also different from the Kubelka–Munk spectrum of azobenzene. Compound **4a** exhibits a strong absorption band with  $\lambda_{\max} = 375$  nm, which is assigned to the  $\pi-\pi^*$  transition, and an unresolved weak absorption band appearing as an inflection at 440 nm, which is assigned to the  $n-\pi^*$  transition. The extension of the  $n-\pi^*$  band of **4a** to 560 nm, which corresponds to the rapid decrease of reflectance from 560 nm in the diffuse

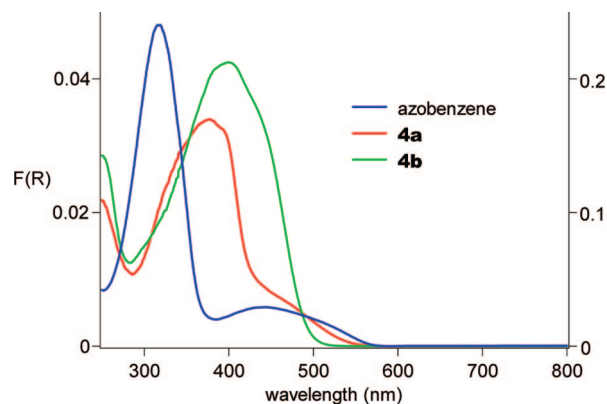


**FIGURE 6.** Kubelka–Munk spectra of azobenzene (blue line), **4a** (red line), and **4b** (green line) in BaSO<sub>4</sub> at room temperature and at the following concentrations: azobenzene, 5 wt %; **4a**, 1 wt %; **4b**, 1 wt %. Barium sulfate was used as a reference in the measurement of the diffuse reflectance spectra. The scales on the left vertical axis correspond to  $F(R)$  of **4a** and **4b**, and those of the right vertical axis correspond to  $F(R)$  of azobenzene.

reflectance spectrum (Figure 5), should be, therefore, responsible for the orange color.

On the other hand, **4b** exhibits a strong absorption band with a maximum at a significantly longer wavelength ( $\lambda_{\max} = 400$  nm), which is assigned to the  $\pi-\pi^*$  transition. The wavelength of its absorption edge is shorter than that of **4a** by ca. 30 nm. This difference is in accord with the fact that the starting wavelength (530 nm) of the rapid decrease in reflectance of **4b** (Figure 5) is significantly shorter than that of **4a** (560 nm). Accordingly, the shorter wavelength of the absorption edge of **4b** corresponds to the absence of the absorption assigned to the  $n-\pi^*$  band of **4b** in the longer wavelength region (530–560 nm). This absence of the  $n-\pi^*$  band in 530–560 nm can be interpreted by blue shift of the  $n-\pi^*$  band, which should lie under the strong  $\pi-\pi^*$  band as in the solution spectra of **4a** and **4b**. A very weak inflection at 440 nm might be interpreted as a superposition of the  $n-\pi^*$  and  $\pi-\pi^*$  bands.<sup>16</sup> The blue shift of the  $n-\pi^*$  band should be due to  $\sigma-\pi^*$  character of the  $n-\pi^*$  band, which results from the formation of the N $\cdots$ Si dative bond. The yellow color of **4b** in the solid state can be, therefore, explained in terms of the blue shift of the  $n-\pi^*$  band. It is to be noted that the  $n-\pi^*$  band plays a dominant role in the solid-state coloration of these compounds, although it is much weaker than the  $\pi-\pi^*$  band.

Azobenzene exhibits the  $\pi-\pi^*$  band at much shorter wavelength ( $\lambda_{\max} = 320$  nm) than **4a** ( $\lambda_{\max} = 375$  nm) and **4b** ( $\lambda_{\max} = 400$  nm). The red shift of the  $\pi-\pi^*$  band in **4b**, where the N $\cdots$ Si dative bond is formed, is considerably larger than that in **4a**, where the N $\cdots$ Si dative bond is not formed. This means that the fluorodiphenylsilyl group induces a substantial bathochromic effect for the  $\pi-\pi^*$  transition inductively and that the formation of the N $\cdots$ Si dative bond further induces a significant bathochromic effect. The  $n-\pi^*$  band of azobenzene ( $\lambda_{\max} = 445$  nm) lies in a wavelength region slightly longer than **4a**. The blue shift of the  $n-\pi^*$  band in **4a** may be due to a substitution effect of the fluorodiphenylsilyl group. The absorption edge of the  $n-\pi^*$  band of azobenzene (590 nm) is

(13) For the application of the chromaticity coordinate in chemistry, see: Harada, J.; Fujiwara, T.; Ogawa, K. *J. Am. Chem. Soc.* **2007**, *129*, 16216–16221.

(14) Kelly, K. L. *J. Opt. Soc. Am.* **1943**, *33*, 627–632.

(15) Diffuse reflectance spectra of powders are usually featureless because both weak and strong absorption bands lead to similar reflectance values. To obtain solution-like absorption spectra, the Kubelka–Munk transformation of diffuse reflectance spectra of highly diluted samples is required. See: (a) Kortüm, G. *Trans. Faraday Soc.* **1962**, *58*, 1624–1631. (b) Kortüm, G.; Braun, W.; Herzog, G. *Angew. Chem., Int. Ed. Engl.* **1963**, *2*, 333–404. (c) Kortüm, G. In *Reflectance Spectroscopy*; Springer: New York, 1969. (d) Fujiwara, T.; Harada, J.; Ogawa, K. *J. Phys. Chem. B* **2004**, *108*, 4035–4038.

(16) It might be also interpreted as a vibrational fine structure. The very weak inflection at 440 nm does not necessarily mean that there is a band,  $\lambda_{\max}$  of which is 440 nm. Even if the inflection is interpreted as a superposition of the  $n-\pi^*$  and  $\pi-\pi^*$  bands, the  $\lambda_{\max}$  of the  $n-\pi^*$  band could be different from 440 nm.

slightly longer than that of **4a** (560 nm). This should be responsible for the deeper color of azobenzene than **4a**.

In summary, the difference in color of **4a**, **4b**, and azobenzene in the solid state was explained by considering the absorption due to the  $n-\pi^*$  transition. In compound **4a**, where the  $N\cdots Si$  dative bond is not formed in the solid state, the  $n-\pi^*$  band appears in the longer wavelength region and results in a deep color. In compound **4b**, where the  $N\cdots Si$  dative bond is formed in the solid state, the  $n-\pi^*$  band with some  $\sigma-\pi^*$  character lies under the strong  $\pi-\pi^*$  band in the shorter wavelength region. As a result, the color of **4b** becomes paler than that of **4a**. The color of azobenzene is deeper than that of **4a**, because the  $n-\pi^*$  band of azobenzene extends to longer wavelength than **4a**. It is thus clearly shown that the difference in color of the powders of **4a** and **4b** does not result from trivial changes in structures owing to packing effects but from essential difference in coordination states.

## Conclusion

We demonstrate here that the  $N\cdots Si$  interaction plays a crucial role in the coloration of disilylazobenzenes in the solid state. Both tetracoordinated and pentacoordinated states of the azobenzenes bearing two fluorodiphenylsilyl groups were successfully isolated by changing the substituents at the 4- and 4'-positions. Their reflectance spectra in the solid state were very different: the pentacoordinated state had a weaker absorbance in the long-wavelength region than the tetracoordinated state, which is ascribed to the shift of the  $n-\pi^*$  transition caused by the  $N\cdots Si$  interaction. This difference in the absorptions due to the  $n-\pi^*$  transition drastically affects the color of the azobenzenes; the color of the pentacoordinated state becomes apparently paler than that of the tetracoordinated state. The  $N\cdots Si$  interactions play a very important role in determining the color of the disilylazobenzenes.

## Experimental Section

**Synthesis of 2,2'-Diiodoazobenzenes 2.**<sup>17</sup> To a toluene solution (100 mL) of 2-iodo-4-methylaniline **1a** (21.0 g, 90.3 mmol) was added manganese dioxide (80 g, 0.92 mol), and the reaction mixture was refluxed for 2.5 h. Filtration of excess manganese dioxide(IV), evaporation of the solvent from the filtrate, separation of the residue by silica-gel chromatography (eluent,  $CHCl_3$ ), and recrystallization from ethanol gave orange crystals of 2,2'-diiodo-4,4'-dimethylazobenzene (**2a**, 9.35 g, 45%). Similarly, 4,4'-dibutyl-2,2'-diiodoazobenzene (**2b**) was synthesized in 20% yield. **2a**: orange crystals, mp 194–196 °C. <sup>1</sup>H NMR (270 MHz,  $CDCl_3$ )  $\delta$  2.37 (s, 6H), 7.21 (d, <sup>3</sup> $J_{HH}$  = 8.0 Hz, 2H), 7.65 (d, <sup>3</sup> $J_{HH}$  = 8.0 Hz, 2H), 7.83 (s, 2H). <sup>13</sup>C NMR (126 MHz,  $CDCl_3$ )  $\delta$  21.2 (CH<sub>3</sub>), 103.8 (C), 117.9 (CH), 130.0 (CH), 140.3 (CH), 143.6 (CMe), 149.1 (CN). Anal. Calcd for C<sub>14</sub>H<sub>12</sub>N<sub>2</sub>I<sub>2</sub>: C, 36.39; H, 2.62; N, 6.06. Found: C, 36.24; H, 2.73; N, 5.86. **2b**: orange crystals, mp 106–108 °C. <sup>1</sup>H NMR (270 MHz,  $CDCl_3$ )  $\delta$  0.94 (t, <sup>3</sup> $J_{HH}$  = 8.0 Hz, 6H), 1.37 (sextet, <sup>3</sup> $J_{HH}$  = 8.0 Hz, 4H), 1.51–1.66 (m, 4H), 2.63 (t, <sup>3</sup> $J_{HH}$  = 8.0 Hz, 4H), 7.23 (dd, <sup>3</sup> $J_{HH}$  = 7.5 Hz, <sup>4</sup> $J_{HH}$  = 1.5 Hz, 2H), 7.67 (d, <sup>3</sup> $J_{HH}$  = 7.5 Hz, 2H), 7.84 (d, <sup>4</sup> $J_{HH}$  = 1.5 Hz, 2H). <sup>13</sup>C NMR (126 MHz,  $CDCl_3$ )  $\delta$  13.9 (CH<sub>3</sub>), 22.3 (CH<sub>2</sub>), 33.2 (CH<sub>2</sub>), 35.0 (CH<sub>2</sub>), 103.8 (C), 117.8 (CH), 129.3 (CH), 139.5 (CH), 148.4 (CBu<sup>n</sup>), 149.0 (CN). Anal. Calcd for C<sub>20</sub>H<sub>24</sub>N<sub>2</sub>I<sub>2</sub>: C, 43.98; H, 4.43; N, 5.13. Found: C, 43.79; H, 4.40; N, 4.98.

**Synthesis of 2,2'-Bis(diphenylsilyl)azobenzenes 3.** To a THF solution (30 mL) of 2,2'-diiodo-4,4'-dimethylazobenzenes (**3a**) (1.00

g, 2.35 mmol) at –105 °C was added *n*-BuLi (1.6 M in hexane, 3.1 mL, 5.0 mmol) rapidly. After the reaction solution was stirred further at –105 °C for 10 min, chlorodiphenylsilane (1.0 mL, 8.0 mmol) was added to it, and the reaction mixture was stirred at room temperature for 12 h. Evaporation of the solvent, separation of the residue by alumina-gel column chromatography (eluent, hexane/ $CHCl_3$ ), and recrystallization from  $CHCl_3$  after evaporation of the eluate gave orange crystals of 2,2'-bis(diphenylsilyl)-4,4'-dimethylazobenzene (**3a**) (0.95 g, 70%). Similarly, 4,4'-dibutyl-2,2'-bis(diphenylsilyl)azobenzene (**3b**) was synthesized in 82% yield. **3a**: orange crystals, mp 227–228 °C. <sup>1</sup>H NMR (400 MHz,  $CDCl_3$ )  $\delta$  2.30 (s, 6H), 5.69 (s, <sup>1</sup> $J_{HSi}$  = 203.6 Hz, 2H), 6.91 (d, <sup>3</sup> $J_{HH}$  = 8.0 Hz, 2H), 7.06 (dd, <sup>3</sup> $J_{HH}$  = 8.0 Hz, <sup>3</sup> $J_{HH}$  = 1.5 Hz, 2H), 7.27–7.36 (m, 14H), 7.76 (dd, <sup>3</sup> $J_{HH}$  = 8.0 Hz, <sup>3</sup> $J_{HH}$  = 1.5 Hz, 8H). <sup>13</sup>C NMR (126 MHz,  $CDCl_3$ )  $\delta$  21.4 (CH<sub>3</sub>), 116.6 (CH), 127.8 (CH), 129.2 (CH), 131.8 (CH), 134.7 (CSi), 135.0 (CSi), 135.7 (CH), 137.9 (CH), 140.5 (CMe), 155.0 (CN). <sup>29</sup>Si NMR (99 MHz,  $CDCl_3$ )  $\delta$  –18.3 (d, <sup>1</sup> $J_{SiH}$  = 203.6 Hz). Anal. Calcd for C<sub>38</sub>H<sub>34</sub>N<sub>2</sub>Si<sub>2</sub>: C, 79.39; H, 5.96; N, 4.87. Found: C, 79.19; H, 5.94; N, 4.72. **3b**: orange crystals, mp 136–137 °C. <sup>1</sup>H NMR (400 MHz,  $CDCl_3$ )  $\delta$  0.86 (t, <sup>3</sup> $J_{HH}$  = 7.5 Hz, 6H), 1.27 (sextet, <sup>3</sup> $J_{HH}$  = 7.5 Hz, 4H), 1.50 (quint, <sup>3</sup> $J_{HH}$  = 7.5 Hz, 4H), 2.51 (t, <sup>3</sup> $J_{HH}$  = 7.5 Hz, 4H), 5.61 (s, <sup>1</sup> $J_{HSi}$  = 202.3 Hz, 2H), 6.88 (d, <sup>3</sup> $J_{HH}$  = 8.0 Hz, 2H), 7.02 (dd, <sup>3</sup> $J_{HH}$  = 8.0 Hz, <sup>3</sup> $J_{HH}$  = 1.5 Hz, 2H), 7.22–7.32 (m, 14H), 7.49 (dd, <sup>3</sup> $J_{HH}$  = 8.0 Hz, <sup>3</sup> $J_{HH}$  = 1.5 Hz, 8H). <sup>13</sup>C NMR (126 MHz,  $CDCl_3$ )  $\delta$  14.0 (CH<sub>3</sub>), 22.4 (CH<sub>2</sub>), 33.4 (CH<sub>2</sub>), 35.5 (CH<sub>2</sub>), 116.8 (CH), 127.8 (CH), 129.3 (CH), 131.1 (CH), 134.84 (CSi), 134.86 (CSi), 135.7 (CH), 137.5 (CH), 145.5 (CBu<sup>n</sup>), 155.2 (CN). <sup>29</sup>Si NMR (99 MHz,  $CDCl_3$ )  $\delta$  –18.8 (d, <sup>1</sup> $J_{SiH}$  = 202.3 Hz). Anal. Calcd for C<sub>44</sub>H<sub>46</sub>N<sub>2</sub>Si<sub>2</sub>: C, 80.19; H, 7.04; N, 4.25. Found: C, 80.06; H, 7.22; N, 4.01.

**Synthesis of 2,2'-Bis(fluorodiphenylsilyl)azobenzenes 4.** To a THF solution (10 mL) of 2,2'-bis(diphenylsilyl)-4,4'-dimethylazobenzene (**3a**) (204 mg, 0.36 mmol) was added AgF (140 mg, 1.01 mmol) at room temperature, and the reaction mixture was stirred for 20 h. After insoluble materials were filtered off through Celite, the filtrate was evaporated. Recrystallization of the residue from  $CHCl_3$  gave orange crystals of 2,2'-bis(fluorodiphenylsilyl)-4,4'-dimethylazobenzene (**4a**) (88.2 mg, 40%). Similarly, 4,4'-dibutyl-2,2'-bis(fluorodiphenylsilyl)azobenzene (**4b**) was synthesized in 79% yield. **4a**: orange crystals, mp 247–248 °C. <sup>1</sup>H NMR (400 MHz,  $CDCl_3$ , 20 °C)  $\delta$  2.32 (s, 6H), 6.90 (d, <sup>3</sup> $J_{HH}$  = 8.0 Hz, 2H), 7.03 (dd, <sup>3</sup> $J_{HH}$  = 8.0 Hz, <sup>3</sup> $J_{HH}$  = 1.5 Hz, 2H), 7.26–7.38 (m, 12H), 7.49 (dd, <sup>3</sup> $J_{HH}$  = 8.0 Hz, <sup>3</sup> $J_{HH}$  = 1.5 Hz, 8H), 7.76 (d, <sup>4</sup> $J_{HH}$  = 1.5 Hz, 2H). <sup>13</sup>C{<sup>1</sup>H} NMR (126 MHz,  $CDCl_3$ , 60 °C)  $\delta$  21.6 (s, CH<sub>3</sub>), 124.0 (s, CH), 127.8 (s, CH), 128.5 (d, <sup>2</sup> $J_{CF}$  = 15.7 Hz, CSi), 129.9 (s, CH), 132.0 (s, CH), 134.3 (d,  $J_{CF}$  = 1.6 Hz, CH), 135.0 (d, <sup>2</sup> $J_{CF}$  = 21.5 Hz, CSi), 137.5 (d,  $J_{CF}$  = 5.0 Hz, CH), 141.9 (s, CMe), 153.1 (s, CN). <sup>19</sup>F NMR (376 MHz,  $CDCl_3$ )  $\delta$  –149.92 (brs). <sup>29</sup>Si{<sup>1</sup>H} NMR (99 MHz,  $CDCl_3$ )  $\delta$  –21.0 (d, <sup>1</sup> $J_{SiF}$  = 270.7 Hz). Anal. Calcd for C<sub>38</sub>H<sub>32</sub>N<sub>2</sub>F<sub>2</sub>Si<sub>2</sub>·0.5H<sub>2</sub>O: C, 73.63; H, 5.37; N, 4.52. Found: C, 73.48; H, 5.47; N, 4.32. **4b**: yellow crystals, mp 136–137 °C. <sup>1</sup>H NMR (400 MHz,  $CDCl_3$ , 20 °C)  $\delta$  0.87 (t, <sup>3</sup> $J_{HH}$  = 7.5 Hz, 6H), 1.30 (sextet, <sup>3</sup> $J_{HH}$  = 7.5 Hz, 4H), 1.54 (quint, <sup>3</sup> $J_{HH}$  = 7.5 Hz, 4H), 2.56 (t, <sup>3</sup> $J_{HH}$  = 7.5 Hz, 4H), 6.89 (d, <sup>3</sup> $J_{HH}$  = 8.0 Hz, 2H), 7.01 (dd, <sup>3</sup> $J_{HH}$  = 8.0 Hz, <sup>3</sup> $J_{HH}$  = 1.5 Hz, 2H), 7.22–7.33 (m, 12H), 7.48 (dd, <sup>3</sup> $J_{HH}$  = 8.0 Hz, <sup>3</sup> $J_{HH}$  = 1.5 Hz, 8H), 7.75 (d, <sup>4</sup> $J_{HH}$  = 1.5 Hz, 2H). <sup>13</sup>C{<sup>1</sup>H} NMR (126 MHz,  $CDCl_3$ , 60 °C)  $\delta$  13.8 (s, CH<sub>3</sub>), 22.5 (s, CH<sub>2</sub>), 33.1 (s, CH<sub>2</sub>), 35.7 (s, CH<sub>2</sub>), 123.6 (s, CH), 127.8 (s, CH), 128.8 (d, <sup>2</sup> $J_{CF}$  = 15.7 Hz, CSi), 129.8 (s, CH), 131.2 (s, CH), 134.4 (s, CH), 134.9 (d, <sup>2</sup> $J_{CF}$  = 20.7 Hz, CSi), 136.7 (d,  $J_{CF}$  = 4.9 Hz, CH), 146.7 (s, CBu<sup>n</sup>), 153.3 (s, CN). <sup>19</sup>F NMR (376 MHz,  $CDCl_3$ )  $\delta$  –150.15 (brs). <sup>29</sup>Si{<sup>1</sup>H} NMR (99 MHz,  $CDCl_3$ )  $\delta$  –20.3 (d, <sup>1</sup> $J_{SiF}$  = 273.3 Hz). Anal. Calcd for C<sub>44</sub>H<sub>44</sub>N<sub>2</sub>F<sub>2</sub>Si<sub>2</sub>: C, 76.04; H, 6.38; N, 4.03. Found: C, 76.05; H, 6.32; N, 3.80.

**Spectral Measurements.** Diffuse UV–vis reflectance spectra were measured on a spectrophotometer equipped with an integrating sphere accessory. For the spectra of nondiluted samples, NaCl powder was ground and used as the reference. For the Kubelka–Munk

(17) Takahashi, H.; Ishioka, T.; Koiso, Y.; Sodeoka, M.; Hashimoto, Y. *Biol. Pharm. Bull.* **2000**, *23*, 1387.

spectra, barium sulfate was ground and used as the diluent and the reference. The ground sample powders and the barium sulfate powder were put in a glass vial and mixed together by rolling and shaking the vial by hand. The mixed powder was used as the sample. Diffuse reflectance spectra were measured and transformed into the Kubelka–Munk spectra using the following equation:

$$F(R) = \frac{(1 - R)^2}{2R} \quad (1)$$

where  $R$  is the observed diffuse reflectance.

**Calculations of Chromaticity Coordinates.** The chromaticity coordinate of a sample under a specific illuminating light can be calculated from the diffuse reflectance spectrum of the sample, the spectrum of the illuminating light, and the spectral sensitivity of the human eye.<sup>6,18</sup> Among these spectra, both the spectrum of the illuminating light, which depends on the lamp used, and the spectral sensitivity of the human eye are given by the Commission International de l'Éclairage (CIE).<sup>19</sup> Therefore, only the diffuse

reflectance spectrum is necessary for the calculation of the chromaticity coordinates. By the use of diffuse reflectance spectra (Figure 5), the chromaticity coordinates for the powder of each of the compounds were calculated.

**Acknowledgment.** We are grateful to Shin-etsu Chemical Co., Ltd., and Tosoh Finechem Corporation for the gift of chlorosilanes and alkyllithiums, respectively. This work was partially supported by Grants-in-Aid for The 21st Century COE Program for Frontiers in Fundamental Chemistry and for Scientific Research from Ministry of Education, Culture, Sports, Science and Technology, Japan. This work was also supported by Grant-in-Aid for Scientific and for Young Scientists by Japan Society for the Promotion of Science. N.K. thanks Foundation Advanced Technology Institute for the financial support.

**Supporting Information Available:** Crystallographic data for **4a** and **4b** in CIF format, compound characterization data, and detailed experiments. This material is available free of charge via the Internet at <http://pubs.acs.org>.

JO801334A

(18) Nassau, K. In *The Physics and Chemistry of Color*, 2nd ed.; John Wiley and Sons, New York, 2001.

(19) CIE Home Page, <http://www.cie.co.at/cie/>.